JOURNAL OF MATERIALS SCIENCE 32 (1997) 2353–2358

Diffusion-based microalloying via reaction sintering

D.P. BISHOP, G.J. KIPOUROS, W.F. CALEY
Technical University of Nova Scotia, P.O. Box 1000, Halifax, Nova Scotia, Canada B3J 2X4

As a possible means of reducing the costs associated with the production of metal matrix composites, the use of inexpensive, naturally occurring minerals as a reinforcing agent is one alternative currently being considered. In such efforts, the occurrence of extensive chemical reaction between the minerals and matrix alloy has been noted. In an effort to utilize the reaction products from such reactions, a novel technique known as core/shell processing was developed. Core/shell and bulk alloy samples were prepared through powder metallurgy techniques (blending, cold isostatic pressing, and sintering) followed by hot swaging and finally machining as required. Sintered samples were examined by means of mercury densitometry, optical/scanning electron microscopy, electron microprobe analysis, and mechanical testing (tensile and impact). Microprobe analysis of sintered core/shell samples indicated the occurrence of extensive chemical reactions between the alloy and mineral particles in the shell region, resulting in a rejection of calcium from the mineral into the surrounding matrix followed by eventual migration into the intergranular regions of the core. Mechanical testing revealed core/shell processed samples had significantly improved impact properties while maintaining tensile properties similar to bulk alloy samples.

1. Introduction

Historically, the most prominent fields of application for metal matrix composites (MMCs) were aerospace and the military, in which cost was generally not a limiting factor [1–3]. However, as costs lowered, applications expanded into commercial aviation and recreational products such as tennis rackets, bicycle frames and golf clubs [3]. Metal-matrix composites have been produced using industrial minerals [4, 5] as reinforcing agents, and similarly, by reaction sintering, ceramic-matrix composites utilizing industrial minerals as reinforcing agents have been fabricated [6, 7]. The industrial mineral used in these cases (wollastonite-$CaSiO_3$) contained calcia as one of the major components.

In most applications for MMCs, the chief concern is weight and because of this, lighter alloys are usually used for the matrix. The primary alloys used for MMCs are aluminium-based. Less frequently, alloys based on titanium, magnesium, copper, iron and nickel are used. Although the name suggests that the matrix is a pure metal, this is in fact rarely the case. Typically, alloying elements are added to aluminium in the order of 1 wt % to achieve the required property alterations. There are, however, several elements that can be added in much lower quantities (0.01–0.1 wt %) and still achieve the required effect. One such element is calcium [8, 9].

Small additions of Ca are known to impart several beneficial effects to aluminium alloys, primarily through intermetallic formation. Since calcium readily combines with Cu and Si to form insoluble intermetallic constituents, a measurable effect on physical properties and behaviour results. By forming insoluble intermetallics with the aforementioned elements, the electrical resistance of aluminium is reduced and mechanical properties improved [8, 9]. Other benefits include improvements in the hot workability of Al–Cu–Mg alloys [10], a reduction in molten alloy surface tension when processing at temperatures above the solidus, and the ability to modify the morphology of secondary phases existing within the bulk alloy. Typically, the amount of calcium added to aluminium alloys is kept low (0.01–2.0 wt %), due to the low solubility of calcium in aluminium (< 0.05 at % at 25 °C) and the detrimental effects on mechanical properties when the calcium content exceeds 2 wt % [8, 9].

In earlier experiments devoted to the sintering behaviour of 2014/wollastonite ($CaSiO_3$) mixtures [11], the occurrence of a chemical reaction between alloy and mineral particles was noted. As a result, calcium was rejected from the mineral into the surrounding alloy, giving rise to the formation of a hard intermetallic, of a composition very similar to that of $CaSi_2Al_2$ [12]. Although such an intermetallic would be expected to improve mechanical properties, the highly porous nature of the sintered product rendered mechanical testing impossible. Thus, in an effort to introduce a calcium-based intermetallic into alloy 2014

0022–2461

using reaction sintering of 2014/wollastonite mixtures, a novel technique was developed. This technique, core/shell processing, utilizes standard powder metallurgy techniques (blending, cold isostatic pressing, sintering, and swaging) to produce a central core of alloy 2014, surrounded by a shell of 2014/ 5v/o wollastonite. Thus, the present study is concerned with the evaluation of the microstructure and mechanical properties of conventionally and core/shell processed alloy samples, with particular attention to the influence of heat treatment.

2. Experimental procedure

2.1. Materials

The two materials used in this work were an aluminium-based alloy, 2014, and an industrial mineral, wollastonite ($CaSiO_3$). The alloy was utilized in a powder form, produced by inert gas atomization, and supplied by Valimet, located in Stockton, CA USA. The powder particles were spherical in nature, having an average particle size of 45 μm. Wrought 2014 is known to have a tensile strength of 205 MPa, and a hardness of 87–98 HRH [13] in the annealed state. The wollastonite (48.3 wt % CaO; 51.7 wt % SiO_2) was mined and beneficiated in Marmora Ontario, Canada [14]. Following beneficiation, the mineral was in a finely divided powdery form, having both fibrous and particulate morphologies, and an average particle size of 15 μm.

2.2. Sample fabrication

The production of the required samples was accomplished using a powder metallurgy (P/M) approach. Initially, the required amounts of mineral and alloy powders were weighed and dry-blended in a ceramic ball mill to ensure a homogenous distribution of the mineral within the mixture. In core/shell sample production, cylindrical green bodies of alloy 2014 were first produced through wet bag pressing in a Loomis™ cold isostatic press (CIP), using a maximum operating pressure of 186 MPa. The resulting green body was then concentrically placed in a larger cylindrical mold, the remaining space filled with the milled alloy/mineral mixture, and re-pressed. To increase the density and improve the mechanical properties of the composite green body, each was subsequently sintered under argon in a quartz tube. Prior to heating, the tube was flushed with industrial grade argon for 5 min, evacuated for 60 min, and then backfilled with argon. While maintaining a continuous flow of argon, the sample was heated to the required temperature (typically 600 °C) and held for a period of time which varied from 30–960 min. Once the required sintering time had elapsed, the sintered product was furnace cooled under argon. This process was repeated for all samples fabricated (approximately 40).

In almost all P/M products, residual porosity exists within sintered bodies. To remove this porosity post sintering operations such as rolling and extrusion are often required [1–3, 15, 16]. Post sintering operations can result in fully dense products and promote metal to metal contact between individual alloy particles [2] resulting in an improved metallurgical bond, and improved mechanical properties. Due to the near net shape processing ability of powder metallurgy, the amount of deformation induced in these operations is often minimal. In attempts to fully densify sintered samples, a hot swaging operation was carried out. For core/shell samples, the porous outer shell was chipped off after sintering and only the remaining core was subjected to the swaging procedure. Prior to swaging each sample was pre-heated at 430 °C for 120 min. Overall, a 60% reduction in area resulted from swaging. After final swaging all samples were water-quenched. The density was measured at each processing stage using mercury densitometry techniques. Finally, alloy samples having either no shell layer or a shell of pressed alloy powder alone, were also prepared through the techniques previously described to provide a means of comparison for the core/shell samples.

2.3. Microstructure examination

To assess sintering behaviour, enhance process optimization, and determine the possible occurrence of interactions between alloy and mineral particles, the sintered microstructures were examined optically using an Olympus BH-2 optical microscope. The presence and/or absence of alloy/mineral interactions was determined by electron probe microanalysis (EPMA) using a Jeol Superprobe.

2.4. Mechanical testing

Further sample characterization involved assessing selected mechanical properties of swaged alloy and core/shell samples using impact and tensile tests. For each test, appropriate sample shapes were machined from swaged rods. As alloy 2014 is heat treatable, mechanical testing was conducted on both annealed and solutionized samples. When annealing, virtually all alloying elements are removed from solution as large precipitates, leaving the alloy in its softest and weakest condition. Solutionizing, however, has the opposite effect, in that the alloying elements (most notably Cu and Mg) are driven into solid solution, thereby dissolving precipitates. In this work, annealed samples were held at 430 °C for 24 h and water quenched, whereas solutionized samples were held at 502 °C for 24 h prior to quenching. Following heat treatment, samples were immediately tested. As a simple means of determining the relative impact properties at 25 °C, a Houndsfield® impact tester was used, whereas relative tensile properties were measured using a Houndsfield® tensometer. Immediately after mechanical testing, the hardness of several samples was measured using a Leco® R600 motorized digital Rockwell hardness tester.

3. Results

3.1. Density measurements

Samples of alloy 2014 were sintered at various temperatures for 30 min and the sintered density measured in

all cases. As shown in Fig. 1, alloy 2014 proved to be responsive to sintering, reaching a maximum sintered density of 97.1 % of theoretical at 600 °C. In an effort to assess the influence of sintering time on final density, alloy samples were sintered at 600 °C for times ranging between 120 and 960 min. Results of these experiments revealed only marginal increases in sintered density, thus deeming a sintering time of 30 min to be adequate. Despite this realization, however, an extended sintering time of 960 min was employed for all alloy and core/shell samples to ensure the occurrence of an appreciable chemical reaction between the mineral and alloy and to promote the migration of reaction products from the shell to core.

3.2. Microstructure examination

Fig. 2 and Table I present the microstructure and EPMA results for alloy 2014 sintered at 600 °C for 960 min. Within the microstructure, intergranular regions (A) were found to consist primarily of Cu and Al together with small amounts of Si, Mn and Mg. Conversely, the alloy grains (B) were found to be of a composition similar to that of the bulk alloy. As well, an Al–Mn–Si–Fe–Cu intermetallic (C), angular and grey in colour, was found evenly scattered throughout the sample. Although it is believed that the intergranular regions (A) are comprised of several phases [17], this identification was beyond the 5 μm resolution of the microprobe available. Hence, a general, overall composition is reported.

For core/shell samples sintered for 960 min at 600 °C, the typical appearance of the microstructure found in the shell is shown in Fig. 3. EPMA results for regions labelled in the figure are presented in Table II. For example, EPMA results indicate that the grey phase (A) is again an Al–Si–Fe–Mn–Cu intermetallic, of essentially identical composition to that previously found in alloy samples. The light grey phase (B) was also found to be an intermetallic, consisting of silicon,

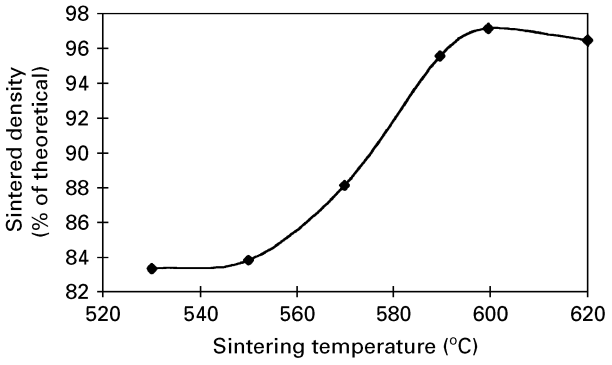

Figure 1 Sintered density versus sintering temperature for aluminium alloy 2014.

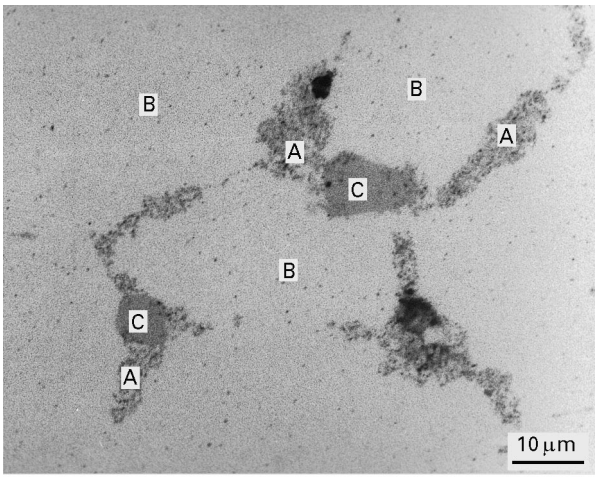

Figure 2 Microstructure of alloy 2014 after sintering for 960 min at 600 °C (intergranular region (A), alloy grains (B), and grey intermetallic (C)).

TABLE I EPMA (wt %) of regions labelled in Fig. 2

Element	Intergranular region (A)	Alloy grains (B)	Grey intermetallic (C)
Si	1.0	0.6	10.0
Al	45.4	96.5	58.5
Fe	–	–	4.6
Mn	1.0	0.3	25.1
Mg	2.2	0.3	0.1
Cu	50.4	2.3	1.7

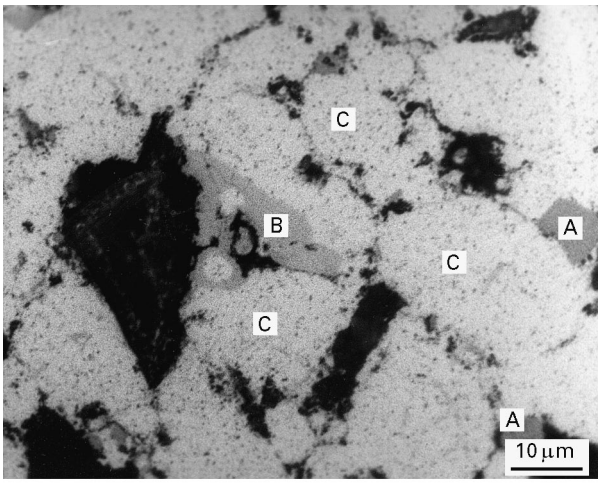

Figure 3 Resulting shell microstructure after sintering for 960 min at 600°C showing the presence of a grey phase (A), light grey phase (B), and alloy grains (C).

TABLE II EPMA results (wt %) for grey (A) and light grey (B) phases, and alloy grains (C) found in shell (Fig. 3) of core/shell sample sintered for 960 min at 600 °C

Element	Grey phase (A)	Light grey phase (B)	Alloy grains (C)
Si	9.5	36.3	0.6
Al	59.0	36.0	96.0
Fe	4.4	–	–
Mn	25.1	0.3	0.2
Mg	–	0.2	0.2
Ca	–	27.2	–
Cu	2.0	–	3.0

aluminium and calcium with trace amounts of other elements, the overall composition in close accordance with that of $CaSi_2Al_2$. Alloy grains (C) were found to have reduced concentrations of alloying elements. EPMA of wollastonite particles exhibiting an outer ring revealed that the mineral was almost completely depleted of lime. Whereas the outer granular ring consisted essentially of alumina and magnesia, the centre was found to be almost pure silica.

The appearance of the core of a core/shell sample is shown in Fig. 4. As labelled in the figure, several dominant features were observed and subjected to EPMA (Table III). These included the presence of a small amount of closed porosity, a grey angular phase (A), intergranular regions (B,C), and alloy grains (D). The grey phase was again found to be an Al–Si–Fe–Mn–Cu intermetallic. The intergranular region, however, was found to consist of at least two different resolvable species grouped together. Of these, one was found to consist primarily of aluminium with small amounts of alloying elements, while the other consisted of essentially aluminium and copper together with a modest amount of magnesium and calcium. Alloy grains were found to have a chemical composition similar to that of the bulk alloy.

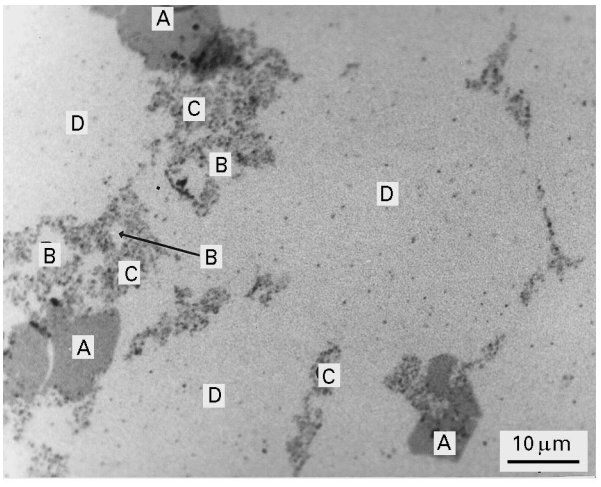

Figure 4 Resulting core microstructure after sintering for 960 min at 600 °C showing the presence of an angular grey phase (A) and intergranular regions (B and C) all surrounded by alloy grains (D).

3.3. Post sintering operations

Sintered samples of alloy 2014 were hot swaged to maximize density. The alloy was found to be highly responsive to swaging, reaching, on average, a density of 98.9 % of theoretical after 60 % reduction in cross-sectional area. In order to compare the behaviour of core/shell samples, the outer shell was removed prior to hot swaging. Core samples were also responsive to this process and reached, on average, a final post-swaged density of 98.7 % of theoretical.

3.4. Mechanical testing

Impact tests were conducted on the cores of core/shell composites and on unmodified alloy samples under a variety of conditions. Such conditions included : (1) sintered, annealed, and quenched, (2) sintered, swaged, annealed and quenched, and (3) sintered, swaged, solutionized and quenched. Results of all samples tested are shown in Table IV. As shown in the table, core samples absorbed a significantly greater amount of energy during the tests than alloy samples, despite similar levels of hardness in all samples. This result was found to be consistent, regardless of the treatments applied prior to testing.

Tensile tests were also performed on both alloy and core/shell samples. All samples were subsequently hot swaged, machined, and heat treated prior to testing. Results of samples tested in the annealed and solutionized state are shown in Table V and in Figs 5 and

TABLE III EPMA results of selected features labelled in Fig. 4 (wt %)

Element	Grey phase (A)	Intergranular region (B)	Intergranular region (C)	Alloy grains (D)
Si	9.9	1.6	1.8	0.8
Al	59.2	90.5	55.2	95.8
Fe	4.1	0.3	–	–
Mn	25.1	2.4	1.6	0.4
Mg	–	2.1	3.4	0.4
Ca	–	–	0.3	–
Cu	1.7	3.1	37.7	2.6

TABLE IV Measured energy absorbed during impact tests and hardness values for alloy and core samples sintered for 960 min at 600 °C

Sample[a]	Heat treatment	Energy absorbed on impact (J)	Hardness (HRE)
Alloy 2014 as-sintered	Annealed	1.6 ± 1.3	44.4 ± 5.0
Alloy 2014 sintered/swaged	Annealed	4.2 ± 0.4	64.6 ± 1.2 (HRH)
Alloy 2014 sintered/swaged	Solutionized	4.5 ± 0.3	106.4 ± 0.6
Core as-sintered	Annealed	4.9 ± 0.3	48.1 ± 5.7
Core sintered/swaged	Annealed	8.5 ± 0.1	62.0 ± 1.9 (HRH)
Core sintered/swaged	Solutionized	9.4 ± 0.5	103.9 ± 0.2

[a]a minimum of two samples were tested in each condition

TABLE V Ductility measurements resulting from tensile tests

Ductility measurement	Alloy sintered for 960 min and swaged		Core sintered for 960 min and swaged	
	Annealed	Solutionized	Annealed	Solutionized
Per cent elongation	12.5 ± 3.5	18.0 ± 7.1	13.2 ± 2.1	21.5 ± 0.7
Per cent reduction in area	11.5 ± 2.1	20.3 ± 7.1	15.2 ± 1.1	30 ± 1.6

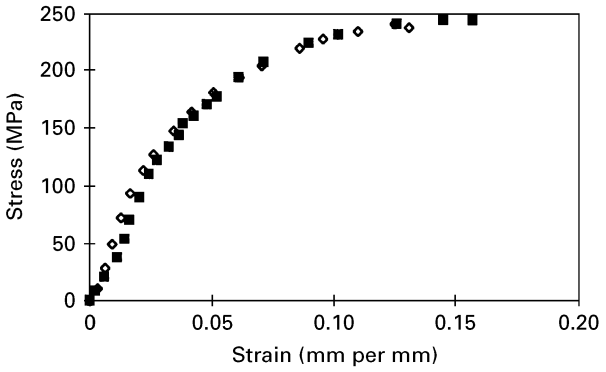

Figure 5 Results of tensile tests conducted on samples annealed prior to testing. key (◇) 2014 standard and (■) core.

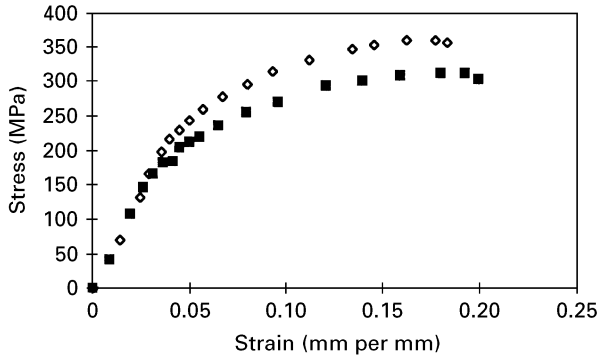

Figure 6 Results of tensile tests on samples solutionized prior to testing. Key; (◇) 2014 standard and (■) core.

6 respectively. As revealed in the figures, core and alloy samples have similar tensile properties in the annealed state, whereas in the solutionized state the ductility of core samples was equivalent or superior to the alloy specimens.

4. Discussion

As previously noted, poor densification of the shell layer occurred during the sintering of core/shell samples. This is the result of a chemical reaction occurring between the alloy and mineral. During such a reaction, oxygen ions are expelled from the wollastonite to the reacting elements (Mg and Al) of the alloy. If the reaction kinetics are not fast enough, some oxygen ions may oxidize the surface of surrounding alloy particles, thereby restricting densification. The fact that the alloy core contains calcium is an indication that the lime component of the wollastonite, despite being a more thermodynamically stable oxide than silica, has evidently been reduced to liberate the oxygen atoms required for the formation of magnesia and alumina. Assuming that these reaction products (magnesia and alumina) have the highest thermodynamic stability of all possible species in the alloy/mineral system, the occurrence of a chemical reaction between the alloy and wollastonite is inevitable. Thus, both the silica and lime in wollastonite would have a tendency to react with the alloy, and the final species may then simply be the result of the competition for the available oxygen. Although no reference to the ionic diffusion of Ca^{2+} and Si^{4+} ions in wollastonite has been reported, in a similar system of calcia, silica and alumina (40/40/20), Ca^{2+} ions are known to have a diffusion rate almost seven times faster than Si^{4+} ions [18]. Assuming a similar situation exists in wollastonite, Ca^{2+} ions would be more readily available for reaction.

Core regions exhibited a structure very similar to alloy samples. The microstructure again contained alloy grains, an intergranular region and an Al–Mn–Si–Fe–Cu intermetallic. However, the intergranular component of the core samples was comprised of two distinguishable species-one rich, and one low in copper. Such behaviour is believed to result from the presence of calcium which has migrated from the shell, into the intergranular regions of the core because of the compositional gradient existing between these two regions. Due to the refining ability of calcium in aluminium alloys, its presence resulted in separation of the intergranular region into two distinct species. The presence of calcium in the intergranular region is not surprising, considering its high affinity for copper and silicon, both of which were concentrated in this region. A final point of interest is the presence of a grey Al–Mn–Si–Fe–Cu intermetallic in both the core and shell regions of core/shell samples. The composition of this phase is similar to that found in alloy 2014 samples sintered for 960 min. Thus, its formation is presumably the result of prolonged alloy sintering, and is seemingly not influenced by the presence of mineral particles.

Given that alloy and core samples were of similar hardness in each of the three test conditions examined (as-sintered, swaged/annealed and swaged/solutionized), one would expect their mechanical properties to also be similar. As this was not the case, microstructural and/or chemical changes are most likely responsible for the observed mechanical behaviour. The primary microstructural difference noted between alloy and core samples was the refinement of the intergranular region in core samples. The most obvious chemical difference was the presence/absence of calcium in core/alloy samples respectively.

In refining the intergranular region, the portion low in alloying element concentration should have superior ductility to that which contains concentrated levels of alloying elements. Thus, conversion of the intergranular region into two species should reduce its brittle nature, and improve ductility. This refinement is also believed to be responsible for the improved impact properties noted in core samples.

5. Conclusions

1. Mixtures of Al 2014/wollastonite were prepared using a novel powder metallurgy technique (core/shell processing) as an attempt to improve selected mechanical properties of the alloy.
2. Using core/shell processing (960 min; 600 °C) calcium is transferred from the shell into aluminium alloy 2014, resulting in microstructural modification. Resulting samples had improved impact properties relative to the unmodified alloy.
3. It is postulated that this improvement was due to the refinement of intergranular regions into two distinct species.

Acknowledgements

Financial assistance provided by the Natural Sciences and Engineering Research Council of Canada (NSERC) through operating grants to two of the authors (W.F.C. and G.J.K.) is gratefully acknowledged.

References

1. Y. B. LIU, S. C. LIM, L.LU and M. O. LAI, *J. Mater. Sci.* **29** (1984) 1999–2007.
2. D. J. LOYD, *Int. Mater. Rev.* **39** (1994) 1–23.
3. M. TAYA and R. J. ARSENAULT, in "*Metal matrix composites*", (Pergamon Press, Toronto, Ontario 1989) pp. 209–237.
4. W. F. CALEY, G. J. KIPOUROS and P. W. KINGSTON, in Proceedings of the 3rd International SAMPE Metals and Metals Processing Conference Toronto, Ontario, Oct. 20–22, 1992, edited by F. H. Froes, W. Wallace, R. A. Cull, and E. Struckholt. (SAMPE, Covina, CA, 1992) **3** M588–599.
5. *Idem. CIM Bull.* **86** (1993) 16.
6. R. H. BRYDEN, E. M. DEVEAU, K. J. KONSZTOWICZ, P. W. KINGSTON and W. F. CALEY, in Proceedings of the Developments and Applications of Ceramics and New Metal Alloys, 32nd CIM Conference of Metallurgists Quebec City, Quebec, edited by R. A. L. Drew and H. Mastaghaci (Canadian Institute of Mining, Metallurgy and Petroleum, Montreal, Quebec, 1993), pp. 357–362.
7. E. M. DEVEAU, R. H. BRYDEN, K. J. KONSZTOWICZ and W. F. CALEY, *Ceramic Engng. Sci. Proc.* **14** (1993) 840.
8. C. L. MANTELL and C. HARDY, in "Calcium metallurgy and technology", (Reinhold, New York, 1979) pp. 35–46.
9. W. A. DEAN, in "Aluminium", Vol. I, edited by K. R. Van Horn, (ASM, Metals Park OH., 1967) pp.163–208.
10. K. T. JACOB and S. SRIKANTH, *High Temp. Mater. Proc.* **9** (1990) 77.
11. D. P. BISHOP, M.A.Sc. thesis, Technical University of Nova Scotia (1995).
12. L. F. Mondolfo, in "*Aluminium alloys*: *structure and properties*", (Butterworth, London, 1976) pp. 460–461.
13. ASM committee on aluminium and aluminium alloys, in "*Metals handbook*", 9th Edn. Vol. 2, (ASM International, Metals Park OH., 1979) pp. 28–43.
14. A. MACKINNON, P. W. KINGSTON and W. F. CALEY, *CIM Bull.* **82** (1989) 617.
15. X. Ni, M. S. MACLEAN and T. N. BAKER, *Mater. Sci. Technol.* **10** (1994) 452.
16. V. V. BHANUPRASAD, R. B. V. BHAT, A. K. KURUVILLA, K. S. PRASAD, A. W. PANDEY, and Y. R. MAHAJAN, *Int. J. Powder Metall.* **27** (1991) 227.
17. G. M. JANOWSKI and B. J. PLETKA, *Metall. Mater. Trans.* **26A** (1995) 3027.
18. G. H. GEIGER and D.R. PORIER, in "*Transport phenomena in metallurgy*", (Addison-Wesley, Don Mills, Ontario, 1973) pp. 431–472.

Received 5 March
and accepted 8 October 1996